JPEDAV (2007) 28:107–114
DOI: 10.1007/s11669-006-9000-y
1547-7037 ©ASM International

Liquid-Solid Phase Equilibria in Metal-Rich Nb-Ti-Hf-Si Alloys

Y. Yang, B. P. Bewlay and Y. A. Chang

(Submitted October 12, 2006)

A thermodynamic description of the Nb-Ti-Hf-Si system is extrapolated from descriptions of the constituent Nb-Ti-Si, Nb-Hf-Si, Hf-Ti-Si, and Nb-Hf-Ti systems using the CALPHAD technique. From this thermodynamic description, the liquidus projection at the metal-rich region of the Nb-Ti-Hf-Si system with the Si concentration up to 40% is calculated. The calculated liquidus surface at this region consists of six primary solidification regions: (Nb), Hf_2Si, $(Hf,Ti)_5Si_3$, $(Nb,Ti)_3Si$, αNb_5Si_3, and βNb_5Si_3. Three five-phase equilibria involving these phases are identified on the liquidus surface by this calculation. They are $L + (Nb) + \alpha Nb_5Si_3 \rightarrow Hf_2Si + (Nb,Ti)_3Si$ at 1814 °C, $L + Hf_2Si + \alpha Nb_5Si_3 \rightarrow (Hf,Ti)_5Si_3 + (Nb,Ti)_3Si$ at 1739 °C, $L + Hf_2Si \rightarrow (Nb) + (Hf,Ti)_5Si_3 + (Nb,Ti)_3Si$ at 1400 °C. To validate the calculated liquidus surface, a total of 10 alloys was directionally solidified. The microstructure of these 10 as-cast alloys was examined by using scanning electron microscopy (back scatter electron (BSE) imaging) and energy dispersive spectrometry (EDS). The solidification simulation of these 10 alloys was then performed by using the Scheil model that is integrated in the multicomponent phase diagram calculation software Pandat. The observed phases presented in the as-cast microstructure of these 10 alloys are in good agreement with those predicted from the Scheil simulation.

Keywords CALPHAD, liquidus surface, multicomponent, phase diagram, phase equilibria, quaternary

1. Introduction

Directionally solidified in situ composites based on niobium and niobium-based silicides are presently being developed for high-temperature structural applications. There has been extensive work on composites generated from binary Nb-Si alloys,[1-5] as well as those with additions such as Ti, Hf, Cr, and Al. Hf and Ti are important alloying additions because they can improve oxidation resistance and strength.[1,2,5,6]. However, there is little previous knowledge of phase equilibria in the Nb-Ti-Hf-Si quaternary system. Many of these Nb-silicide-based composites are generated by liquid-solid processing techniques.[5,6] Thus, knowledge of the Nb-Ti-Hf-Si liquidus surface is required in order to predict the phase content and volume fractions of phases in these in situ composites. Obtaining such knowledge exclusively from experiments is cumbersome and expensive. Thermodynamic modeling of multi-component systems using the CALPHAD approach has been shown to be a very efficient tool in this regard.[7] In previous studies, we had developed thermodynamic descriptions of the Hf-Ti-Si,[8] Nb-Ti-Hf,[9] Nb-Ti-Si[9] and Nb-Hf-Si[10] systems. The objective of the present study is to develop a thermodynamic description for the metal-rich region of the Nb-Ti-Hf-Si system through the extrapolation of its constituent ternaries. Then combining the calculated liquidus surface and solidification paths with the experimental evidence, the liquidus surface of the metal-rich end of the Nb-Ti-Hf-Si system can be described.

This article was presented at the Multi-Component Alloy Thermodynamics Symposium sponsored by The Alloy Phase Committee of the joint EMPMD/SMD of the Minerals, Metals, and Materials Society (TMS), held in San Antonio, Texas, March 12-16, 2006, to honor the 2006 William Hume-Rothery Award recipient, Professor W. Alan Oates of the University of Salford, UK. The symposium was organized by Y. Austin Chang of the University of Wisconsin, Madison, WI, Patrice Turchi of the Lawrence Livermore National Laboratory, Livermore, CA, and Rainer Schmid-Fetzer of the Technische Universitat Clausthal, Clauthal-Zellerfeld, Germany.

Y. Yang, CompuTherm LLC, 437 S. Yellowstone Dr., Madison, WI 53719; **B. P. Bewlay,** General Electric Company, GE Global Research Center, 1 Research Circle, Niskayuna, NY 12309; **Y. A. Chang,** Department of Materials Science and Engineering, University of Wisconsin-Madison, Madison, WI 53706. Contact e-mail: yang@chorus.net

2. Background on Liquidus Surface of the Constituent Ternaries

2.1 Hf-Ti-Si

Figure 1 shows the calculated liquidus projection of the Hf-Ti-Si system by Yang et al.[8] In the region close to the Hf-Ti binary for Si concentrations between 0 and 30 at.%, there are three primary solidification phases: (Nb), Hf_2Si, and $(Hf,Ti)_5Si_3$. Both Ti_5Si_3 in Ti-Si binary and Hf_5Si_3 in Hf-Si binary are considered to be one phase $(Hf,Ti)_5Si_3$ in the Hf-Ti-Si and Nb-Ti-Hf-Si systems. The Hf_2Si with Ti

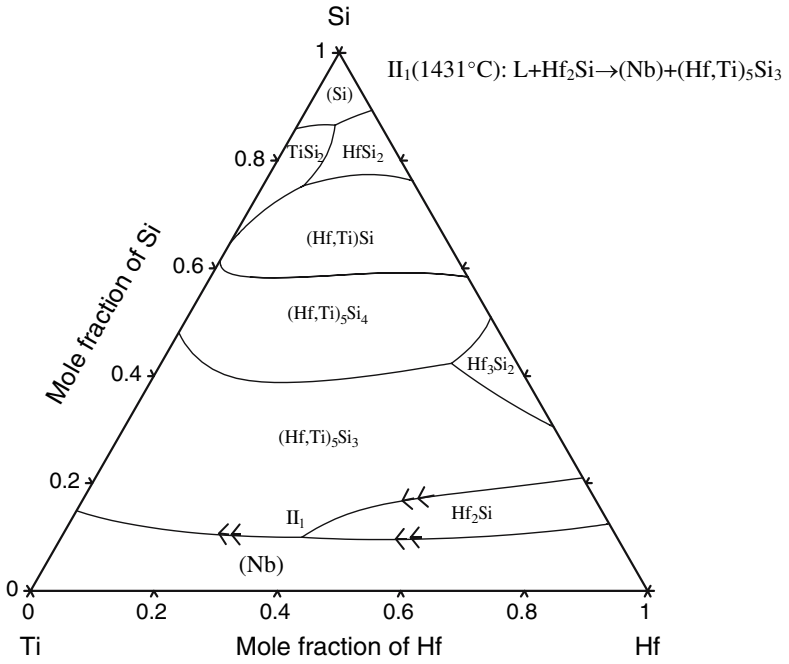

Fig. 1 The calculated liquidus projection of Hf-Ti-Si [8]

in solid solution is referred to as Hf_2Si, and (Nb) refers to the ternary solid solution of Hf, Ti and Si with the bcc_A2 structure. The denotation of the phase names is explained in Table 1, which also lists the Pearson symbols and thermodynamic models used.

A eutectic groove extends from the L $\rightarrow$ (Nb) + Hf_2Si in the Hf-Si binary to the L $\rightarrow$ (Nb) + $(Hf,Ti)_5Si_3$ in the Ti-Si binary. Because of the different binary eutectic reactions there is a change in the nature of the liquidus surface, and the eutectic groove, with decreasing Hf and increasing Ti concentration. The invariant reaction that corresponds to the change on the eutectic groove involves four phases, i.e. liquid, (Nb), Hf_2Si and $(Hf,Ti)_5Si_3$. According to Rhines,[11] this phase transition is a class II reaction of the form L + Hf_2Si $\rightarrow$ (Nb) + $(Hf,Ti)_5Si_3$, denoted by II_1. The calculated temperature and liquid composition of this reaction are 1431 °C and Hf-51Ti-9.9Si, respectively. They are in good agreement with the measured temperature 1420 ± 20 °C and the estimated liquid composition Hf-50Ti-9.5Si reported by Bewlay et al.[12]

2.2 Nb-Ti-Si

The Nb-Ti-Si system has been thermodynamically modeled by Liang and Chang[13] Recently, Yang et al. remodeled this system by considering newly reported experimental data.[14,15] Figure 2 shows the calculated liquidus projection of the Nb-Ti-Si system by Yang.[9] In the region close to the Nb-Ti binary for Si concentrations up to 30 at.%, there are five primary solidification phases: (Nb), Ti_5Si_3, $(Nb,Ti)_3Si$, αNb_5Si_3, and βNb_5Si_3. Since the concentration and temperature range of the βNb_5Si_3 primary solidification region has negligible contribution to liquid-solid phase equilibria of the metal-rich region of the Nb-Ti-Hf-Si system, it will not be discussed in this paper. Both Nb_3Si and Ti_3Si have Pearson symbol of *t*P32 and is referred to as $(Nb,Ti)_3Si$. Ti_5Si_3 refers to Ti_5Si_3 with Nb in solid solution. The αNb_5Si_3 with Ti in solid solution is referred to as αNb_5Si_3. (Nb) refers to the ternary solid solution of Nb, Ti and Si with the bcc_A2 structure.

Two class II invariant reactions II_2 and II_3 exist in the metal-rich region of the liquidus projection. Symbol II_2 in Fig. 2 denotes the invariant reaction L + αNb_5Si_3 $\rightarrow$ Ti_5Si_3 + $(Nb,Ti)_3Si$. The calculated temperature and liquid composition of this reaction are 1615°C and Nb-55.6Ti-18.3Si, respectively. This reaction is experimentally reported to occur at between 1600 and 1650 °C with a composition of Nb-66Ti-19Si by Bewlay et al.[14] Symbol II_3 in Fig. 2 denotes the invariant reaction L + $(Nb,Ti)_3Si$ $\rightarrow$ (Nb) + Ti_5Si_3 with calculated temperature and composition being 1352 °C and Nb-76.6Ti-14.5Si, respectively. Bewlay et al.[14] reported that this reaction occurs at a temperature of ~1350 °C with a composition of Nb-76Ti-13.5Si. The calculated results reasonably agree with the experimental measurements. Yang[9] also performed solidification simulation for alloys in this region. The simulation results can well account for the experimentally observed as-cast microstructure. Therefore, the calculated liquidus projection of Nb-Ti-Si in Fig. 2 can be reliably used to construct the Nb-Ti-Hf-Si quaternary liquid-solid phase equilibria in the metal-rich region.

2.3 Nb-Hf-Si

Figure 3 shows the calculated liquidus projection of the Nb-Hf-Si system by Yang et al.[10] In the region close to the Nb-Hf binary for Si concentrations up to 30 at%, there are

Table 1 Primary solidification phases at the metal-rich region of the Nb-Ti-Hf-Si system

Phase symbol	Thermodynamic model	Pearson symbol	Phase description
Hf-Ti-Si			
(Nb)	(**Hf**,**Ti**,Si)$_1$(Va)$_3$	*c*I2	Ternary solid solution with the bcc_A2 structure
Hf_2Si	(**Hf**,Ti)$_2$Si	*t*I12	Ternary solid solution based on the Hf_2Si
$(Hf,Ti)_5Si_3$	(**Hf**,**Ti**)$_5$Si$_3$	*h*P16	Ternary solid solution based on the Hf_5Si_3 and Ti_5Si_3
Ti_3Si	(Hf,**Ti**)$_3$Si	*t*P32	Ternary solid solution based on the Nb_3Si and Ti_3Si
Nb-Ti-Si			
(Nb)	(**Nb**,**Ti**,Si)$_1$(Va)$_3$	*c*I2	Ternary solid solution with the bcc_A2 structure
Ti_5Si_3	(Nb,**Ti**)$_5$Si$_3$	*h*P16	Ternary solid solution based on the Ti_5Si_3
$(Nb,Ti)_3Si$	(**Nb**,**Ti**)$_3$Si	*t*P32	Ternary solid solution based on the Nb_3Si and Ti_3Si
αNb_5Si_3	(**Nb**,Ti) $_5$Si$_3$	*t*I32	Ternary solid solution based on the low temperature form of Nb_5Si_3(D8*l*)
βNb_5Si_3	(**Nb**,Ti) $_5$Si$_3$	*t*I32	Ternary solid solution based on the high temperature form of Nb_5Si_3(D8*m*)
Nb-Hf-Si			
(Nb)	(**Nb**,**Hf**,Si)$_1$(Va)$_3$	*c*I2	Ternary solid solution with the bcc_A2 structure
Hf_2Si	(Nb,**Hf**)$_2$Si	*t*I12	Ternary solid solution based on the Hf_2Si
Hf_5Si_3	(Nb,**Hf**)$_5$Si$_3$	*h*P16	Ternary solid solution based on the Hf_5Si_3
Nb_3Si	(**Nb**,Hf)$_3$Si	*t*P32	Ternary solid solution based on the Nb_3Si
αNb_5Si_3	(**Nb**,Hf) $_5$Si$_3$	*t*I32	Ternary solid solution based on the low temperature form of Nb_5Si_3(D8*l*)
βNb_5Si_3	(**Nb**,Hf) $_5$Si$_3$	*t*I32	Ternary solid solution based on the high temperature form of Nb_5Si_3(D8*m*)
Nb-Ti-Hf-Si			
(Nb)	(**Nb**,**Hf**,**Ti**,Si)$_1$(Va)$_3$	*c*I2	Quaternary solid solution with the bcc_A2 structure
Hf_2Si	(Nb,**Hf**,Ti)$_2$Si	*t*I12	Quaternary solid solution based on the Hf_2Si
$(Hf,Ti)_5Si_3$	(Nb,**Hf**,**Ti**)$_5$Si$_3$	*h*P16	Quaternary solid solution based on the Hf_5Si_3 and Ti_5Si_3
$(Nb,Ti)_3Si$	(**Nb**,Hf,**Ti**)$_3$Si	*t*P32	Quaternary solid solution based on the Nb_3Si and Ti_3Si
αNb_5Si_3	(**Nb**,Hf,Ti) $_5$Si$_3$	*t*I32	Quaternary solid solution based on the low temperature form of Nb_5Si_3(D8*l*)
βNb_5Si_3	(**Nb**,Hf,Ti) $_5$Si$_3$	*t*I32	Quaternary solid solution based on the high temperature form of Nb_5Si_3(D8 *m*)

Note: The T element in bold font is the major element in that sublattice

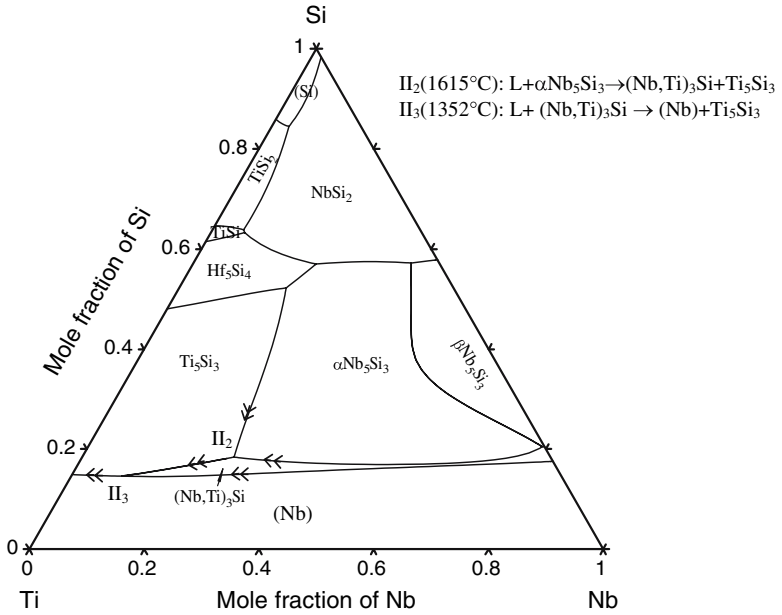

Fig. 2 The calculated liquidus projection of Nb-Ti-Si [8]

six primary solidification phases: (Nb), Hf_2Si, Hf_5Si_3, Nb_3Si, αNb_5Si_3, and βNb_5Si_3. As mentioned above, βNb_5Si_3 is not considered in this paper. The Hf_5Si_3 and Hf_2Si refer to Hf_5Si_3 and Hf_2Si with Nb in the solid solution. The Nb_3Si and αNb_5Si_3 with Hf in the solid solutions are referred to as Nb_3Si and αNb_5Si_3, respectively.

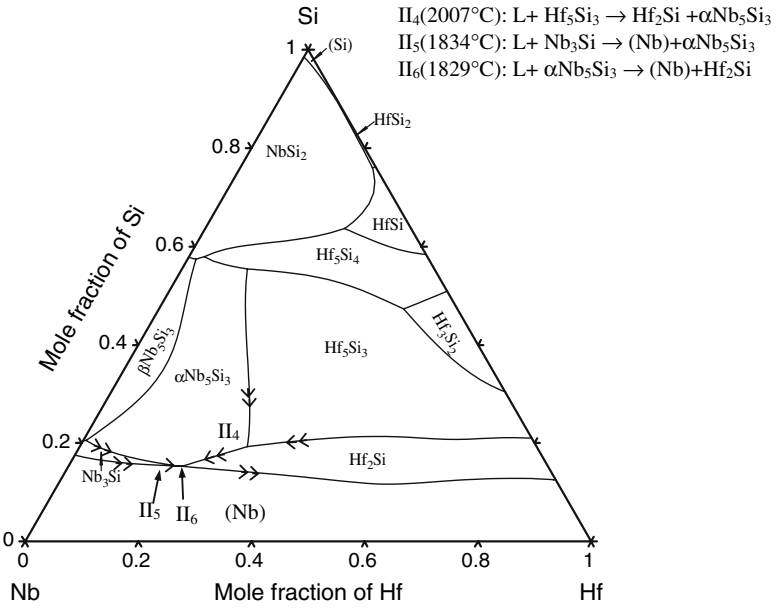

Fig. 3 The calculated liquidus projection of Nb-Hf-Si [10]

(Nb) refers to the ternary solid solution of Nb, Hf, and Si with the bcc_A2 structure.

There are three class II invariant reactions in this portion of liquidus projection: II_4, II_5, and II_6. Symbol II_4 denotes the invariant reaction $L + Hf_5Si_3 \rightarrow Hf_2Si + \alpha Nb_5Si_3$. The calculated temperature and liquid composition of this reaction are 2007 °C and Nb-30Hf-19Si, respectively. Symbol II_5 denotes the invariant reaction $L + Nb_3Si \rightarrow (Nb) + \alpha Nb_5Si_3$ with calculated temperature and composition of 1834 °C and Nb-19Hf-15Si, respectively. Symbol II_6 denotes the invariant reaction $L + \alpha Nb_5Si_3 \rightarrow (Nb) + Hf_2Si$ with the calculated temperature and composition being 1829 °C and Nb-20Hf-15Si, respectively. A comparison between the calculated results and the estimated values for these three reactions was performed by Yang et al.[10] Most of the calculated values are in good agreement with the estimated values except for the II_5 reaction. The four-phase equilibrium $L + \alpha Nb_5Si_3 \rightarrow (Nb) + Nb_3Si$ proposed by Bewlay et al.[11] is different from the calculated result $L + Nb_3Si \rightarrow (Nb) + \alpha Nb_5Si_3$. Due to the shallow nature of this part of liquidus surface it is difficult to be certain about the precise nature of the reaction. However, both of above reactions were considered to be possible, within the uncertainty of the experimental measurements and the thermodynamic modeling. This liquidus projection is used in constructing the liquid-solid phase equilibria of the Nb-Ti-Hf-Si system in the metal-rich region.

2.4 Nb-Hf-Ti

The Nb-Hf-Ti system has been thermodynamically modeled by Yang.[9] The liquidus surface of this system is simple and there is only one primary solidification phase of (Nb), a ternary solid solution of Nb-Hf-Ti with the bcc_A2 structure.

3. Experimental and Thermodynamic Modeling Procedures

The samples for this study were directionally solidified using cold crucible directional solidification[1,4] after triply melting the starting charges from high-purity elements (>99.99%). The compositions that were investigated are shown in Table 2. They were chosen based on prior work on the constituent ternaries and are of technological importance.[16] The directional solidification procedure has been described in more detail previously.[1,6] Typically at least two samples were generated for each composition. Mass losses were measured after preparation of each sample and they were found to be less that 0.1 wt.%. The total interstitial levels of the elements used was less than 1000 weight ppm (C, O, and N). All of the samples were examined using scanning electron microscopy (back scatter electron (BSE) imaging) and energy dispersive spectrometry (EDS).

All four constituent binaries of the Nb-Ti-Hf-Si system have been thermodynamically modeled. In the present modeling, the thermodynamic parameters of the Hf-Ti-Si, Nb-Ti-Si, Nb-Hf-Si, and Nb-Hf-Ti ternary systems are taken from literature.[8-10] Neither experimental nor calculated thermodynamic property data for the Nb-Ti-Hf-Si quaternary system were found in literature. Therefore, the thermodynamic description of the Nb-Ti-Hf-Si system is obtained by extrapolation from its constituent ternaries. Pandat[17] was used to calculate the phase diagrams and solidification paths.

Table 2 Comparison between the phases observed from as-cast alloys and those predicted from Scheil simulation

		Phases predicted from Scheil simulation	
Alloy composition	**Phases observed from as-cast alloys**	**Name**	**Mole fraction**
Nb-7.5Hf-21Ti-16Si	(Nb), $(Nb,Ti)_3Si$	**(Nb)**	0.39
		$(Nb,Ti)_3Si$	0.59
		$(Hf,Ti)_5Si_3$ (a)	0.02
Nb-10Hf-21Ti-16Si	(Nb), $(Nb,Ti)_3Si$	**(Nb)**	0.39
		$(Nb,Ti)_3Si$	0.58
		$(Hf,Ti)_5Si_3$ (a)	0.03
Nb-12.5Hf-21Ti-16Si	(Nb), $(Nb,Ti)_3Si$	**(Nb)**	0.39
		$(Nb,Ti)_3Si$	0.57
		$(Hf,Ti)_5Si_3$ (a)	0.04
Nb-7.5Hf-33Ti-16Si	(Nb), $(Nb,Ti)_3Si$	**(Nb)**	0.4
		$(Nb,Ti)_3Si$	0.55
		$(Hf,Ti)_5Si_3$ (a)	0.05
Nb-10Hf-33Ti-16Si	(Nb), $(Nb,Ti)_3Si$	**(Nb)**	0.41
		$(Nb,Ti)_3Si$	0.54
		$(Hf,Ti)_5Si_3$ (a)	0.05
Nb-12.5Hf-33Ti-16Si	(Nb), $(Nb,Ti)_3Si$,$(Hf,Ti)_5Si_3$	**(Nb)**	0.41
		$(Nb,Ti)_3Si$	0.52
		$(Hf,Ti)_5Si_3$	0.07
Nb-8Hf-25Ti-12Si	(Nb), $(Nb,Ti)_3Si$	**(Nb)**	0.56
		$(Nb,Ti)_3Si$	0.4
		$(Hf,Ti)_5Si_3$ (a)	0.04
Nb-8Hf-25Ti-14Si	(Nb), $(Nb,Ti)_3Si$	**(Nb)**	0.48
		$(Nb,Ti)_3Si$	0.49
		$(Hf,Ti)_5Si_3$ (a)	0.03
Nb-8Hf-25Ti-16Si	(Nb), $(Nb,Ti)_3Si$	**(Nb)**	0.4
		$(Nb,Ti)_3Si$	0.57
		$(Hf,Ti)_5Si_3$ (a)	0.03
Nb-8Hf-25Ti-18Si	(Nb), $(Nb,Ti)_3Si$	**(Nb)**	0.35
		αNb_5Si_3	0.06
		$(Nb,Ti)_3Si$	0.56
		$(Hf,Ti)_5Si_3$ (a)	0.03
Nb-8Hf-25Ti-20Si	(Nb), $(Nb,Ti)_3Si$, αNb_5Si_3	**(Nb)**	0.31
		αNb_5Si_3,	0.16
		$(Nb,Ti)_3Si$	0.5
		$(Hf,Ti)_5Si_3$ (a)	0.03
Nb-8Hf-25Ti-22Si	(Nb), $(Nb,Ti)_3Si$, αNb_5Si_3	**(Nb)**	0.28
		αNb_5Si_3,	0.26
		$(Nb,Ti)_3Si$	0.43
		$(Hf,Ti)_5Si_3$ (a)	0.03

Note: (a) denotes that the mole fraction of the phase is no more than 0.05. The phases in bold font are those phases present in both the Scheil and equilibrium simulation

4. Results and Discussions

4.1 Liquidus projection

Figure 4 shows a calculated three-dimensional tetrahedron of liquidus projection at the metal-rich region of Nb-Ti-Hf-Si, with Si concentration up to 40 at.%. The three side faces of the tetrahedron are Nb-Ti-Si, Nb-Hf-Si, and Hf-Ti-Si, respectively. The base of the tetrahedron is Nb-Hf-Ti. The primary-phase regions and invariant reactions in these four constituent ternaries have been discussed individually in Section 2. The details of the liquid-solid phase equilibria within the Nb-Ti-Hf-Si quaternary system are discussed below.

As described in Section 2, II_1~II_6 are invariant reactions in the Nb-Ti-Si, Nb-Hf-Si, and Hf-Ti-Si systems and they are four-phase equilibria. All the reactions throughout this paper are under a constant pressure of one atm. When these ternaries are combined with Nb-Hf-Ti to form the quaternary system, one more degree of freedom is introduced. These ternary invariant reactions thus become monovariant

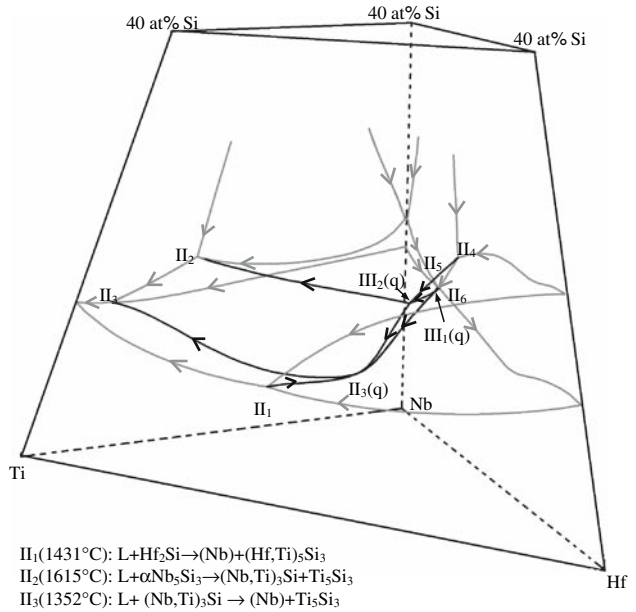

Fig. 4 The calculated liquidus projection at the metal-rich region of Nb-Ti-Hf-Si with the black lines as monovariant reactions in the quaternary and the grey lines as monovariant reactions in the constituent ternary systems

reactions in the quaternary, i.e. reaction with one degree of freedom. The compositions of the liquid for these monovariant reactions, L + solid$_1$ + solid$_2$ + solid$_3$, emanate from their constituent ternary invariant points, i.e. II_1~II_6. They are shown in Fig. 4 as black lines within the tetrahedron to differentiate them from those ternary monovariant lines in gray. Encompassed by ternary and quaternary mono-variant lines, six primary phases (Nb), Hf_2Si, αNb_5Si_3, $(Nb,Ti)_3Si$, $(Hf,Ti)_5Si_3$ and βNb_5Si_3 exist in this tetrahedron. Each ternary monovariant reaction (gray line) is associated with two primary phases. Similarly, each quaternary monovariant reaction (black line) is associated with three primary phases. For instance, the monovariant line $III_2(q)$-II_2 is associated with $(Hf,Ti)_5Si_3$, $(Nb,Ti)_3Si$, and αNb_5Si_3.

At the intersection of four quaternary monovariant lines forms a five-phase equilibrium that is invariant in a quaternary systems. Three invariant reactions have been identified by calculation in the metal-rich region of the Nb-Ti-Hf-Si quaternary. They are denoted by $III_1(q)$, $III_2(q)$, and $II_3(q)$ with the symbol (q) indicating that they are for the quaternary system. $III_1(q)$ denotes the reaction L + (Nb) + αNb_5Si_3 → Hf_2Si + $(Nb,Ti)_3Si$ occurring at 1814 °C. According to Rhines,[11] this reaction is class III five-phase equilibrium. For this type of reaction, two tie-tetrahedra descending from higher temperature join to form an isothermal tie-hexahedron (L + (Nb) + Hf_2Si + (Nb, $Ti)_3Si$ + αNb_5Si_3) which then divides into three tie-tetrahedra that continue to lower temperatures. The two tie-tetrahedra above the transition temperature: L + (Nb) + $(Nb,Ti)_3Si$ + αNb_5Si_3 and L + (Nb) + Hf_2Si + αNb_5Si_3 emanate from II_5 and II_6 in the Nb-Hf-Si system. Of the three tie-tetrahedra below the transition temperature, one forms a solid-state equilibrium (Nb) + Hf_2Si + $(Nb,Ti)_3Si$ + αNb_5Si_3, and the other two involves liquid, i.e. L + Hf_2Si + $(Nb,Ti)_3Si$ + αNb_5Si_3 and L + (Nb) + Hf_2Si + $(Nb,Ti)_3Si$ will continue to solidify until reaching invariant reactions $III_2(q)$ and $II_3(q)$, respectively.

The reaction denoted by $III_2(q)$ is L + Hf_2Si + αNb_5Si_3 → $(Hf,Ti)_5Si_3$ + $(Nb,Ti)_3Si$, which occurs at 1739 °C. It is also class III five-phase equilibrium. The two tie-tetrahedra above the transition temperature are L + Hf_2Si + $(Nb,Ti)_3Si$ + αNb_5Si_3 and L + Hf_2Si + $(Hf,Ti)_5Si_3$ + αNb_5Si_3. The former one descends from the reaction $III_1(q)$ and the latter one descends from the invariant reaction II_4 in the Nb-Hf-Si ternary. The three tie-tetrahedra below the invariant temperature are L + $(Hf,Ti)_5Si_3$ + $(Nb,Ti)_3Si$ + αNb_5Si_3, L + Hf_2Si + $(Hf,Ti)_5Si_3$ + $(Nb,Ti)_3Si$, and Hf_2Si + $(Hf,Ti)_5Si_3$ + $(Nb,Ti)_3Si$ + αNb_5Si_3. The former two tie-tetrahedra involving liquid continue to solidify until reaching II_2 in the Nb-Ti-Si binary and $II_3(q)$ in the Nb-Ti-Hf-Si quaternary, while the last one is a solid-state equilibrium which is stable down to room temperature. $II_3(q)$ denotes a class II five-phase equilibrium L + Hf_2Si → (Nb) + $(Hf,Ti)_5Si_3$ + $(Nb,Ti)_3Si$ in the Nb-Ti-Hf-Si system. According to Rhines,[11] for this type of reaction, three tie-tetrahedra descend from higher temperature and join to form an isothermal tie-hexahedron, L + (Nb) + Hf_2Si + $(Hf,Ti)_5Si_3$ + $(Nb,Ti)_3Si$, which then splits into two tie-tetrahedra that continue to lower temperatures. The three tie-tetrahedra above the invariant temperature are L + Hf_2Si + $(Hf,Ti)_5Si_3$ + (Nb, $Ti)_3Si$, L + (Nb) + Hf_2Si + $(Nb,Ti)_3Si$, and L + (Nb) + Hf_2Si + $(Hf,Ti)_5Si_3$, coming from $III_1(q)$, $III_2(q)$, and II_1, respectively. The two tie-tetrahedra below the invariant temperature are L + (Nb) + $(Hf,Ti)_5Si_3$ + $(Nb,Ti)_3Si$ and (Nb) + Hf_2Si + $(Hf,Ti)_5Si_3$ + $(Nb,Ti)_3Si$. The former tie-tetrahedra involving liquid continue to solidify until reaching II_3 in the Nb-Ti-Si binary. The latter one is a solid-state four-phase equilibrium. The detailed reaction scheme drawn from the calculated results is illustrated in Fig. 5.

4.2 Solidification Simulation

A total of 12 quaternary alloys were cast in this study. As-cast microstructures of these alloys were characterized using scanning electron microscopy (back scatter electron (BSE) imaging) and energy dispersive spectrometry (EDS). Solidification path simulations were performed using the Scheil[18] and equilibrium models. The Scheil model assumes no diffusion in the solid, uniform liquid composition, and thermodynamic equilibrium at liquid-solid interface. The equilibrium model assumes complete mixing in the liquid and solid, and complete thermodynamic equilibrium between solid and liquid. Both models require thermodynamic information only and have been integrated into the solidification simulation module of Pandat.[17] These two models represent two extreme cases of solidification. Using the alloy Nb-8Hf-25Ti-22Si as an example,

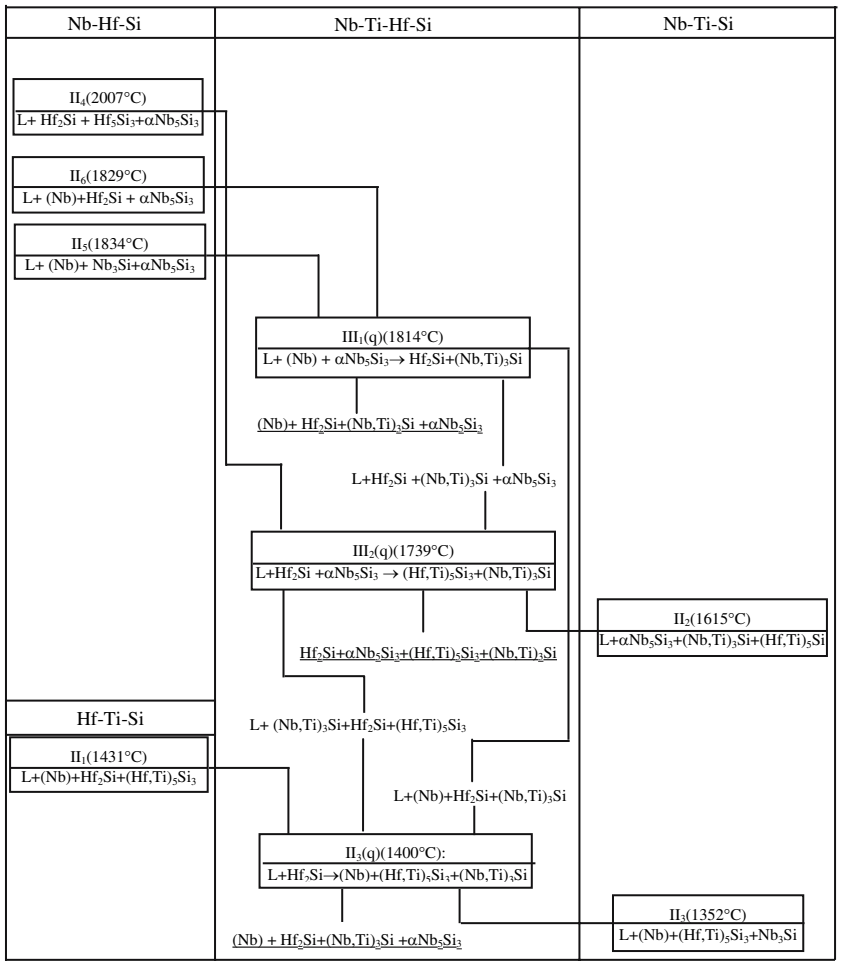

Fig. 5 The reaction scheme of Nb-Ti-Hf-Si in the metal-rich region

typical simulation results using these two models are presented in Fig. 6(a). The phases predicted by equilibrium simulation are αNb_5Si_3, $(Nb,Ti)_3Si$, and (Nb), while those predicted by Scheil simulation are αNb_5Si_3, $(Nb,Ti)_3Si$, (Nb), and $(Hf,Ti)_5Si_3$. The experimental observation of (Nb), $(Nb,Ti)_3Si$, and αNb_5Si_3 in Fig. 6(b) is consistent with both the equilibrium and Scheil simulation results. However, the mole fractions of (Nb), $(Hf,Ti)_5Si_3$, $(Nb,Ti)_3Si$, and αNb_5Si_3 from the Scheil simulation are qualitatively closer to the experimental observation. The absence of $(Hf,Ti)_5Si_3$ in the experimental observation is probably due to its small amount beyond the detection limit. Similar comparisons were also obtained for the remaining 11 alloys. Comparisons between predicted phases by the equilibrium and Scheil solidification simulations and the observed phases in as-cast alloys are summarized in Table 2. The experimentally observed phases are generally predictable within the two boundaries of the Scheil and equilibrium simulations.

5. Conclusions

A thermodynamic description of the Nb-Ti-Hf-Si system is extrapolated from descriptions of the constituent Nb-Ti-Si, Nb-Hf-Si, Hf-Ti-Si and Nb-Hf-Ti systems using the CALPHAD technique. From this thermodynamic description, the liquidus projection in the metal-rich region of the Nb-Ti-Hf-Si system with the Si concentrations up to 40% is calculated. The calculated liquidus surface is associated with six primary solidification regions: (Nb), Hf_2Si, $(Hf,Ti)_5Si_3$, $(Nb,Ti)_3Si$, αNb_5Si_3, and βNb_5Si_3. Three five-phase equilibria involving in these phases are identified on the liquidus surface. They are $III_1(q)$: $L + (Nb) + \alpha Nb_5Si_3 \rightarrow Hf_2Si + (Nb,Ti)_3Si$ at 1814 °C, $III_2(q)$: $L + Hf_2Si + \alpha Nb_5Si_3 \rightarrow (Hf,Ti)_5Si_3 + (Nb,Ti)_3Si$ at 1739 °C, and $II_3(q)$: $L + Hf_2Si \rightarrow (Nb) + (Hf,Ti)_5Si_3 + (Nb,Ti)_3Si$ at 1400 °C.

The sequence of invariant reactions suggests that the liquidus surface in the metal-rich region of the Nb-Ti-Hf-Si system descends from the Nb-Hf-Si ternary to the Nb-Ti-Si ternary. The lowest temperature of solidification in this region ends with $L \rightarrow (Nb) + Ti_5Si_3$ in the Nb-Ti-Si system. To validate the calculated liquidus surface, a total of 12 alloys was directionally solidified. The microstructures of these 12 as-cast alloys were examined by using scanning electron microscopy (back scatter electron (BSE) imaging) and energy dispersive spectrometry (EDS). The observed phases presented in the as-cast microstructure of these 12 alloys are in accordance with those predicted from

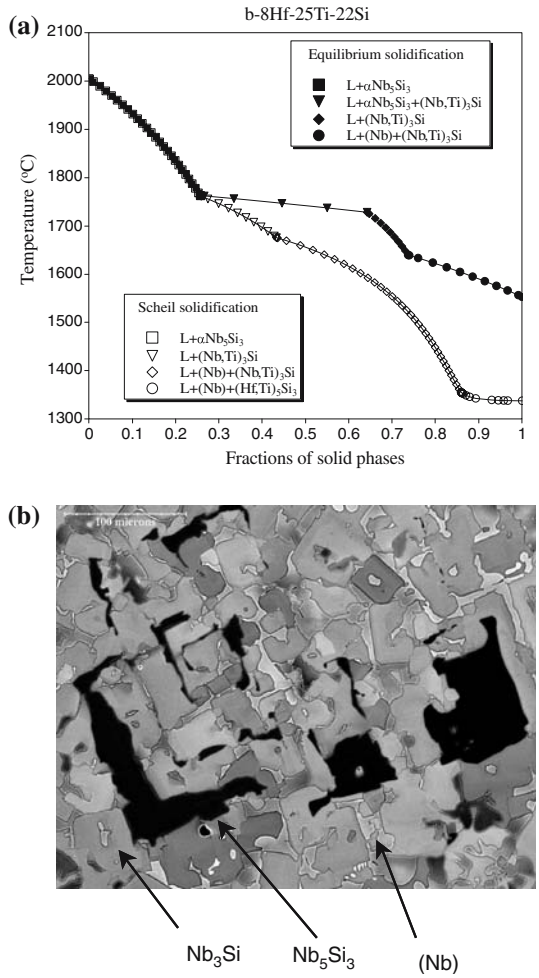

Fig. 6 (a) Calculated solidification path of Nb-8Hf-25Ti-22Si using the Scheil and equilibrium model. (b) A BSE image of as-cast Nb-8Hf-25Ti-22Si alloy.

the Scheil simulation. This suggests that the topological features of the currently proposed liquidus surface in the metal-rich region of the Nb-Ti-Hf-Si system are correct. Additional experiments are needed for validation of the compositions and temperatures of the invariant reactions $III_1(q)$, $III_2(q)$ and $II_3(q)$. The calculated phase diagram in this work can serve as a guide to select the alloy compositions for further experimental investigation.

Acknowledgements

The authors would like to thank D. J. Dalpe for performing directional solidification experiments.

References

1. B.P. Bewlay, M.R. Jackson, and P.R. Subramanian, Processing High-temperature Refractory-metal Silicide In-situ Composites, *JOM-US*, 1999, **51**(4), p 32-36
2. B.P. Bewlay, M.R. Jackson, and H.A. Lipsitt, The Balance of Mechanical and Environmental Properties of a Multi-element Niobium-Niobium Silicide-based In situ Composite, *Metall. Mater. Trans. A.*, 1996, **27A**(12), p 3801-3808
3. M.G. Mendiratta, J.J. Lewandowski, and D.M. Dimiduk, Strength and Ductile-Phase Toughening in the Two-Phase Niobium/Niobium Silicide (Nb5Si3) Alloys, *Metall. Mater. Trans. A.*, 1991, **22A**(7), p 1573-1583
4. M.R. Jackson, B.P. Bewlay, R.G. Rowe, D.W. Skelly, and H.A. Lipsitt, High-temperature Refractory Metal-Intermetallic Composites, *JOM-US*, 1996, **48**(1), p 39-44
5. P.R.Subramanian, M.G. Mendiratta, and D.M. Dimiduk, Microstructures and Mechanical Behavior of Nb-Ti Base beta + silicide Alloys, *MRS Proceedings*, 322, High Temperature Silicides and Refractory Alloys, 1994, p 491-502
6. B.P. Bewlay, M.R. Jackson, W.J. Reeder, and H.A. Lipsitt, Microstructures and Properties of DS In-situ Composites of Nb-Ti-Si Alloys, *MRS Proceedings*, 364, High-Temperature Ordered Intermetallic Alloys, VI, Pt. 2, 1995, p 943-948
7. X.-Y. Yan, Y.A. Chang, Y. Yang, F.-Y. Xie, S.-L. Chen, F. Zhang, S. Daniel, and M.-H. He, A Thermodynamic Approach for Predicting the Tendency of Multicomponent Metallic Alloys for Glass Formation, *Intermetallics*, 2001, **9**(6), p 535-538
8. Y. Yang, B.P. Bernard, and Y.A. Chang, Thermodynamic Modeling of the Hf-Ti-Si System, submitted to Intermetallics, 2006
9. Y. Yang, Private Communication, CompuTherm LLC, 437S, Yellowstone Dr., Suite 217, Madison, WI 53719, 2005
10. Y. Yang, Y.A. Chang, J.-C. Zhao, and B.P. Bewlay, Thermodynamic Modeling of the Nb-Hf-Si Ternary System, *Intermetallics*, 2003, **11**(5), p 407-415
11. F.N. Rhines, *Phase Diagrams in Metallurgy - Their Development and Application*. McGraw-Hill, London, 1956
12. B.P. Bewlay, M.R. Jackson, Y. Yang, and Y.A. Chang. Liquid-Solid Phase Equilibria in Metal-rich Hf-Ti-Si Alloys, Submitted to *Z. Metallkd.*, 2006
13. H. Liang and Y.A. Chang, Thermodynamic Modeling of the Nb-Si-Ti Ternary System, *Intermetallics*, 1999, **7**(5), p 561-570
14. B.P. Bewlay, M.R. Jackson, and H.A. Lipsitt, The Nb-Ti-Si Ternary Phase Diagram: Evaluation of Liquid-Solid Phase Equilibria in Nb- and Ti-rich Alloys, *J. Phase Equilib. Diff.*, 1997, **18**(3), p 264-278
15. B.P. Bewlay, M.R. Jackson, and R.R. Bishop, The Nb-Ti-Si Ternary Phase Diagram: Determination Of Solid-State Phase Equilibria in Nb- and Ti-rich alloys, *J. Phase Equilib. Diff.*, 1998, **19**(6), p 577-586
16. B.P. Bewlay, S.D. Sitzman, L.N. Brewer, and M.R. Jackson, Analyses of Eutectoid Phase Transformations in Nb-Silicide In situ Composites, *Microsc. Microanal.*, 2004, **10**, p 1-11
17. S.-L. Chen, F. Zhang, S. Daniel, Y.A. Chang, X.-Y. Yan, F.-Y. R. Xie Schmid-Fetzer, and W.A. Oates, The Pandat Software Package and its Applications, *CALPHAD*, 2002, **26**, p 175-188
18. E. Scheil, Unbroken Series of Solid Solutions in the Binary Systems of the Elements, *Z. Metallkd.*, 1942, **34**, p 242-246
19. B.P. Bewlay, R.R. Bishop, and M.R. Jackson, The Nb-Hf-Si Ternary Phase Diagram. Liquid-Solid Phase Equilibria in Nb-and Hf-Rich Alloys, *Z. Metallkd.*, 1999, **90**(6), p 413-422